

Provided for non-commercial research and education use.
Not for reproduction, distribution or commercial use.



(This is a sample cover image for this issue. The actual cover is not yet available at this time.)

This article appeared in a journal published by Elsevier. The attached copy is furnished to the author for internal non-commercial research and education use, including for instruction at the authors institution and sharing with colleagues.

Other uses, including reproduction and distribution, or selling or licensing copies, or posting to personal, institutional or third party websites are prohibited.

In most cases authors are permitted to post their version of the article (e.g. in Word or Tex form) to their personal website or institutional repository. Authors requiring further information regarding Elsevier's archiving and manuscript policies are encouraged to visit:

<http://www.elsevier.com/copyright>

Contents lists available at [SciVerse ScienceDirect](#)

Journal of Theoretical Biology

journal homepage: www.elsevier.com/locate/yjtbi

The fine art of surfacing: Its efficacy in broadcast spawning

Jan Moláček^{a,1}, Mark Denny^{b,2}, John W.M. Bush^{a,1,*}

^a Department of Mathematics, Massachusetts Institute of Technology, 77 Massachusetts Avenue, Cambridge, MA 02139, USA

^b Hopkins Marine Station of Stanford University, Pacific Grove, CA 93950, USA

ARTICLE INFO

Article history:

Received 27 May 2011

Received in revised form

5 October 2011

Accepted 11 October 2011

Available online 19 October 2011

Keywords:

Reproductive strategy

Mathematical model

Encounter rate

Random walk

External fertilization

ABSTRACT

Many organisms reproduce by releasing gametes into the surrounding fluid. For some such broadcast spawners, gametes are positively or negatively buoyant, and, as a result, fertilization occurs on a two-dimensional surface rather than in the bulk of the air or water. We here rationalize this behaviour by considering the encounter rates of gametes on the surface and in the fluid bulk. The advantage of surfacing is quantified by considering an infinitely wide body of water of constant depth. Differential loss rates at the surface and in the bulk are considered and their influence on the robustness of surface search assessed. For small and moderate differential loss rates, the advantage of surfacing is very robust and significant; only for large loss rate differences can the advantage of surfacing be nullified.

© 2011 Elsevier Ltd. All rights reserved.

1. Introduction

Sexual reproduction in both plants and animals often involves broadcasting gametes into a fluid environment, either air or water. In some such broadcast spawners (notably, red algae, terrestrial plants, and a wide sampling of marine invertebrates) male propagules (either pollen or sperm) are released into the fluid and make their way to the eggs retained by females. More commonly, both sperm and eggs are released, and fertilization occurs in the fluid. Unlike animals that copulate – for whom the motility of the adult is used to ensure that sperm meets egg – few reproductive propagules of broadcast spawners are sufficiently motile to control their position in the environment. Instead, they move at the whim of wind or currents. The resulting random transport can be advantageous – it allows for mating among widely dispersed or sedentary individuals – but it also poses a serious challenge. Because random mixing causes dilution of propagules, through time the likelihood decreases that sperm and egg will meet (Denny, 1988; Denny and Shibata, 1989). Even in still water, the effective rotational diffusion of small motile gametes causes them to move randomly (Berg, 1993).

At least two obvious strategies are available to broadcast spawners to maximize their probability of fertilization in the presence of random mixing. First, species that release both male

and female propagules should spawn synchronously in response to either chemical or environmental cues, thereby increasing the initial concentration of gametes. This strategy is commonplace among marine invertebrates and seaweeds (e.g. Pearse et al., 1988; Levitan and Petersen, 1995; Togashi and Cox, 2001; Santelices, 2002). Second, organisms should minimize the spatial domain in which gametes move, thereby increasing their encounter rates. For example, some seaweeds living in tide pools release gametes only at low tide when the pool is isolated from the sea (Pearson and Brawley, 1996). Other broadcast spawners take advantage of the coherent structures in the turbulent field, which confine their gametes to relatively thin filament sheets (Crimaldi and Browning, 2004). A more general implementation of this second strategy (“surfacing”) constrains propagules to a surface rather than allowing them to mix through a volume. Gametes in water could be positively buoyant, for example, leading to confinement at the water’s surface. Alternatively, negative buoyancy in water leads to confinement near the seafloor or lake bed. In air, the negative buoyancy of pollen grains tends to concentrate them near the ground (Denny, 1994).

While it would seem intuitively obvious that confining the search for a mate to a plane provides an advantage, there are several complications to consider. First, the risk of death might be higher near the surface than in the fluid bulk. The seafloor, for example, is densely covered with a variety of suspension feeders all too willing to consume reproductive propagules, and rainfall and the resulting decrease in sea-surface salinity can kill buoyant gametes of corals (Harrison et al., 1984). Moreover, the delay and perils associated with traveling to a surface might conceivably make it faster and safer to remain in the bulk fluid. Under what

* Corresponding author. Tel.: +1 857 991 9280; fax: +1 617 253 8911.

E-mail addresses: molacek@math.mit.edu (J. Moláček), mwdenny@stanford.edu (M. Denny), bush@math.mit.edu (J.W.M. Bush).

¹ Developed the mathematical model.

² Provided the biological background and references.

circumstances is surfacing a viable reproductive strategy? We here provide a quantitative comparison between encounter rates at surfaces and in the bulk, and so rationalize and quantify the evolutionary advantage of surfacing.

The results are applicable to numerous scenarios covering a wide range of scales, including biofilms, puddles, ponds, lakes, oceans, and the atmosphere. Examples abound. A thin liquid film is required for sexual reproduction of liverworts, hornworts, mosses and ferns, in order for the antherozoids (the equivalent of sperm) to be able to reach neighbouring egg cells. In eelgrass (genus *Vallisneria*), male flowers detach from the plant and float up to the surface while the female flowers rise to the surface by straightening their coiled stalks. After successful pollination, the stalks coil down again and the fruit develops underwater. Aquatic plants of genera *Lepilaena*, *Ruppia*, *Halodule* and others (Cox and Knox, 1988) live in coastal waters or brackish lakes and release flowers that float to the water surface, where they rupture and expel pollen which then floats on the surface until colliding with a stigma. Several species of corals on the Great Barrier Reef release buoyant gamete bundles that float to the surface and then break apart, releasing eggs and sperm (Harrison et al., 1984).

We will model the movement of all such gametes as a random walk (Cox, 1983). By that we specifically mean movement consisting of discrete steps of constant length δ in a random direction happening over a constant timescale τ , resulting in an effective diffusivity $D \approx \delta^2/\tau$. This provides a good model of particle motion in many biological settings. Small passive particles, like the gametes of red algae in calm water, may be moved about by the random motion of surrounding molecules and the resulting Brownian motion is a quintessential example of a random walk. Motile small cells, i.e. flagellated sperm or their equivalent, can be separated into two types according to their mode of propulsion. Cells of the first type “run and tumble”, abruptly changing direction after some approximately constant time interval within which they swim along straight lines, hence the relevance of the random walk model. Cells of the second type do not run and tumble, but the direction of their movement changes frequently due to random impacts with surrounding molecules. The impact rate gives us the typical timescale over which the direction of movement is constant, beyond which velocities are uncorrelated. The random walk also provides a simple model for particles being advected and dispersed by ambient turbulence. The characteristic time and lengthscales T and L are prescribed by those of the turbulent vortices, and the effective turbulent diffusivity is given by $D \approx L^2/T$. The rate at which the gametes are dispersed at the surface and in the fluid bulk may also vary due to anisotropic turbulence; for example, turbulence in the near surface region may be marked by larger horizontal than vertical turbulent eddies. We thus extend our model to include the possibility of an anisotropic random walk. Regardless of their mode of transport, gametes senesce, die, and may be consumed by predators, and our model includes the effects of the rate at which gametes are lost from the system.

Motivated by an interest in intercellular molecular transport and olfactory sensing in insects, Adam and Delbrück (1968) compared the relative efficiency of two-dimensional and three-dimensional diffusive searches, assuming uniform initial distribution of particles and convenient circular boundaries. In contrast to their approach, we use encounter probabilities instead of mean diffusion times to compare the two scenarios, which enables us to consider the influence of gamete mortality, planar boundaries and point-like initial gamete distribution.

In Section 2, we present the idealized model for the surface and bulk search scenarios. We then present a means of comparing the two scenarios quantitatively using encounter probabilities and derive exact formulae for these probabilities using a simple model of

random walk and gamete mortality. In Section 3, we compare the encounter probabilities in the two scenarios. We first consider the case in which the environmental conditions are the same on the surface and in the bulk, and then the more general case, in which there may be a larger loss rate or more vigorous turbulent mixing near the surface. We deduce the critical water depth at which the surface search become advantageous relative to the bulk search. Furthermore, we consider the influence of anisotropic diffusion on the advantage gained by surfacing. Finally, in Section 4 we apply the results to three typical real-world scenarios, and discuss the implications of our results and the limitations of our approach.

2. The model

Consider an organism living in a body of water of constant finite depth H and infinite horizontal extent. We suppose that its sexual reproduction involves encounters between male gametes and female gametes, where at least one of the gametes is moving, either passively or actively. If the sum of typical radii of the male and female gametes is r_T , we can model the male gametes as point particles while the female gametes can be represented by a sphere (or, in 2D, a circle) of radius r_T . Henceforth, we shall refer to the male gametes as “particles” and the female gametes as “targets”. Successful encounter occurs when the particle touches the surface of the target. We assume that the organisms are distributed uniformly across the bottom surface of the water body and that each organism releases the same number of targets (female gametes). The number of particles (male gametes) released by each organism does not impact the differential encounter probability of surface and bulk searches; therefore we consider the encounter probability of a single particle. Note that our model is not restricted to the case of a female gamete being much larger than the male, as r_T represents the sum of the gamete radii and so applies equally well to the case of isogamy.

To model the loss of viable gametes due to predation, energy depletion, senility or other causes, we introduce the loss rate λ . We assume that λ is constant, that is, the probability of a given gamete dying during a small time interval δt is $\lambda \delta t$. Such an approximation is appropriate when predation is the primary cause of gamete mortality, and adopted here in general for the sake of mathematical simplicity. Since the gametes are generally different in size and motility, we expect the loss rates to be different for different sexes. Therefore we denote by λ_1 and λ_2 the target and particle loss rates, respectively. As we shall demonstrate below in Section 2.1, only the total loss rate $\lambda = \lambda_1 + \lambda_2$ will enter into our calculations. We assume the gametes are released simultaneously from multiple points distributed uniformly long the water's lower or upper surface. This corresponds to the simultaneous gamete release by bottom-dwelling or surface-dwelling organisms, respectively.

There are two reproductive strategies available to the organisms: either they can release their gametes onto a surface (the water surface or the bottom) or into the water bulk. We will compare the two reproductive strategies using the gamete encounter probability. The encounter probability P_S will be the probability that a particle (male gamete) introduced randomly onto a plane uniformly filled with points simultaneously releasing N targets (female gametes) each, will be successful in encountering at least one target before it dies. Similarly, P_B will be the encounter probability for a particle introduced into the water bulk of constant depth H , whose bottom surface is again uniformly filled with target-releasing points. If the average density of the organisms per unit area is ρ_0 and each organism releases N targets, then if the targets are released onto the surface, their surface density will be $\rho_S = N\rho_0$.

2.1. Encounter probability

It is our aim to determine the encounter probabilities P_S and P_B of a single particle with targets released from uniform planar distribution of points, on the surface and in the bulk, respectively. A good starting point is to consider a simpler scenario – the case of one particle and one target, in an infinite d -dimensional space (so that no boundaries need to be considered). Suppose that the target has size r_T and is originally a distance R from the particle. Then the encounter probability \bar{P}_d will be a function of r_T , the loss rates λ_1, λ_2 and distance R only. For $d=2,3$, that is for search on a surface or in an infinite fluid bulk, we can find \bar{P}_d exactly. In Appendix A we derive the following formulae:

$$\bar{P}_2(R, r_T, \kappa_S) = \frac{K_0(R/\kappa_S)}{K_0(r_T/\kappa_S)}, \tag{1}$$

$$\bar{P}_3(R, r_T, \kappa_B) = \frac{r_T \exp\{r_T/\kappa_B\}}{R \exp\{R/\kappa_B\}}, \tag{2}$$

where $K_0(s)$ is the modified Bessel function of the second kind of order 0, $\kappa_S = \sqrt{D_S/\lambda_S}$ and $\kappa_B = \sqrt{D_B/\lambda_B}$. Here λ_S, λ_B and D_S, D_B are the total loss rates and diffusivities on the surface and in the bulk, respectively. κ_S and κ_B can be interpreted as the typical distances a gamete travels before dying, on the surface and in the bulk, respectively, and will be henceforth referred to as the gamete's range. In each region the total loss rate $\lambda = \lambda_1 + \lambda_2$ and the diffusivity $D = (\delta_1^2 + \delta_2^2)/(2d\tau)$ is a constant associated with the gamete random walk with steplengths δ_1, δ_2 for each gamete and common time-step τ . By definition, \bar{P}_2 and \bar{P}_3 are equal to 1 for $R = r_T$, and then rapidly decrease. For large R they decrease roughly exponentially. Fig. 2 illustrates the dependence of \bar{P}_2 and \bar{P}_3 on the nondimensional distance R/κ for two values of r_T/κ , when $\kappa_S = \kappa_B = \kappa$. We observe that $\bar{P}_2 > \bar{P}_3$ for $R > r_T$, \bar{P}_3 decreases faster than \bar{P}_2 with the initial gamete distance R/κ , and the difference between the two probabilities increases with decreasing r_T/κ , so smaller target size makes surface search more advantageous compared to fluid bulk search.

Since in our 3D scenario we work with a body of finite depth only, we now consider the case of one particle and one target originally a distance R apart on the bottom surface, in a body of water of constant depth H (see Fig. 1 with $h=0$). Denote the encounter probability in this scenario by \bar{P}_{3F} . In Appendix B we derive the formula

$$\bar{P}_{3F}(R, r_T, \kappa_B, H) = \frac{A(R/\kappa_B, H/\kappa_B)}{A(r_T/\kappa_B, H/\kappa_B)}, \tag{3}$$

where

$$A(x, y) = \sum_{n \in \mathbb{Z}} \frac{\exp\{-\sqrt{x^2 + 4n^2 y^2}\}}{\sqrt{x^2 + 4n^2 y^2}}.$$

Now that we know \bar{P}_2 and \bar{P}_{3F} – the single-particle, single-target encounter rates – it is straightforward to derive P_S and P_B , the single-particle, multiple-target encounter rates, since we

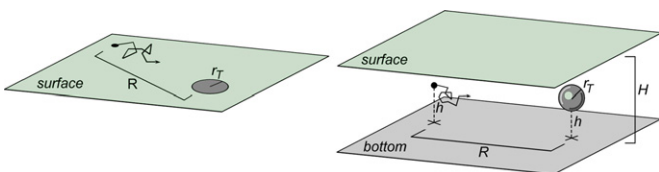


Fig. 1. Idealized model of a gamete searching for a mate on a water surface (left) and in the fluid bulk (right). The female gamete is represented by a circular or spherical target of radius r_T , while the male gamete is modelled as a point particle. The body of water has a constant depth H in the 3D scenario.

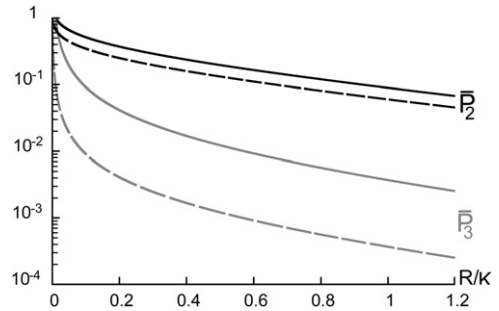


Fig. 2. Graphs of the encounter probabilities $\bar{P}_2(R, r_T, \kappa)$ and $\bar{P}_3(R, r_T, \kappa)$ as functions of the relative distance R/κ , on a semi-logarithmic scale, for (a) $r_T/\kappa = 0.01$ and (b) $r_T/\kappa = 0.001$. R is the initial distance between gametes and $\kappa = \sqrt{D/\lambda}$ the gamete range, where λ is the loss rate and D the diffusivity. Both \bar{P}_2 and \bar{P}_3 decrease exponentially with R/κ for large R/κ , with \bar{P}_3 decreasing at a faster rate. By definition of the encounter distance r_T , we must have $\bar{P}_2(r_T) = \bar{P}_3(r_T) = 1$. Comparing the two graphs indicates that having a smaller target size r_T increases the difference between the two probabilities, and so increases the advantage of surface search.

Table 1

List of the symbols used in this paper. Subscripts S and B denote values on the surface and in the bulk, respectively.

Symbol	Definition	Symbol	Definition
D, D_S, D_B	Gamete diffusivity	$\lambda, \lambda_S, \lambda_B$	Gamete loss rate
P_S, P_B	Gamete encounter probability	$\kappa, \kappa_S, \kappa_B$	Gamete range
r_T	Target size	r	Relative target size
H	Water depth	\bar{H}	Relative water depth
ρ_S	Target density	$\bar{\rho}$	Nondim. target density
		$\mu = \kappa_S/\kappa_B$	Relative bulk hostility

know the original target density ρ_S and hence also the probability of finding a target release point at a distance R (Table 1). Integrating over all possible distances R we obtain (see Appendix C)

$$P_S(\rho_S, r_T, \kappa_S) = 1 - \exp\left\{-\rho_S \int_{r_T}^{\infty} 2\pi R \bar{P}_2(R) dR\right\}, \tag{4}$$

$$P_B(\rho_B, r_T, \kappa_B) = 1 - \exp\left\{-\rho_B \int_{r_T}^{\infty} 2\pi R \bar{P}_{3F}(R) dR\right\}, \tag{5}$$

where \bar{P}_2 and \bar{P}_{3F} are defined by Eqs. (1) and (3), respectively. Evaluating the integrals in Eqs. (4) and (5) yields

$$P_S(\rho_S, r_T, \kappa_S) = 1 - \exp\{-\rho_S \kappa_S^2 I_1(r_T/\kappa_S)\}, \tag{6}$$

$$P_B(\rho_B, H, r_T, \kappa_B) = 1 - \exp\{-\rho_B \kappa_B^2 I_2(r_T/\kappa_B, H/\kappa_B)\}, \tag{7}$$

where $I_1(s) = 2\pi/K_0(s) \int_s^{\infty} x K_0(x) dx$, and $I_2(s, t) = 2\pi/A(s, t) \int_s^{\infty} x A(x, t) dx$. The encounter probabilities P_S, P_B are proportional to target density ρ_S when ρ_S is small. With increasing target density they converge exponentially to 1. P_B is proportional to r_T for small target size r_T , whereas P_S is proportional to $1/\ln(1/r_T)$, so target size plays a smaller role in the surface than the bulk searches.

3. Comparison of surface and bulk encounter probabilities

We proceed by comparing encounter probabilities on the surface and in the bulk. In Section 3.1, we consider the case in which the conditions on the surface and in the bulk are equally favourable, that is, the loss rates and gamete motilities are equal. In Section 3.2, we consider the more general case of unequal loss rates and motilities, and derive an expression for the critical water depth at which the surface and fluid bulk searches are

equally advantageous. Finally, in Section 3.3, we consider the case of anisotropic diffusion and show that it can be included in our model by suitable rescaling of parameters.

3.1. Equal loss rates and motilities at the surface and in the bulk

Suppose that both the loss rate and the gamete motility are the same on the surface and in the bulk. Then $\kappa_S = \sqrt{D/\lambda} = \sqrt{(\delta_1^2 + \delta_2^2)/4\lambda\tau}$ while $\kappa_B = \sqrt{(\delta_1^2 + \delta_2^2)/6\lambda\tau} = \sqrt{4/6}\kappa_S$, from the definition of diffusivity D (see Appendix A), where δ_1, δ_2 are the length scales associated with the random walk of each type of gamete, and τ is the associated time-step. Let us write $\kappa = \kappa_S$, so $\kappa_B = \kappa/\sqrt{1.5}$. Writing $\bar{\rho} = \rho_S\kappa^2$, $r = r_T/\kappa$ and $\bar{H} = H/\kappa$ for the nondimensional target density, target size and water depth, respectively, Eqs. (6) and (7) transform to

$$P_S(\bar{\rho}, r) = 1 - \exp\{-\bar{\rho}I_1(r)\}, \quad (8)$$

$$P_B(\bar{\rho}, r, \bar{H}) = 1 - \exp\left\{-\frac{\bar{\rho}}{1.5}I_2(\sqrt{1.5}r, \sqrt{1.5}\bar{H})\right\}. \quad (9)$$

Since $r = r_T/\kappa$ is the ratio of target radius to the gamete's range, we expect this to be a small parameter, $r \ll 1$. When the loss rate and gamete motility are the same for the surface and bulk searches, the only reason that P_S and P_B differ is that the bulk provides a larger region for the gametes; equivalently, the average spacing between male and female gametes is less at the surface. Therefore we must have $P_S > P_B$ for all $\bar{H} > 0$.

Now we can visualize the advantage of the surface search by plotting the ratio of P_S/P_B as a function of $\bar{\rho}$ for various values of r and \bar{H} . The results are shown in Fig. 3. For large target densities, the ratio P_S/P_B tends to 1, since with increasing target density, both P_S and P_B must tend to 1 separately: the particle is bound to encounter a target for sufficiently high target density. We also observe that the convergence of P_S/P_B to 1 happens for increasingly large target densities $\bar{\rho}$ as we increase the relative depth \bar{H} , because a larger total number of targets is required to fill a larger volume with sufficiently high density. Conversely, for small target densities $\bar{\rho}$, the ratio P_S/P_B is independent of target density and proportional to \bar{H} .

3.2. Unequal loss rates and motilities at the surface and in the bulk

We now determine the conditions under which $P_S > P_B$. Combining Eqs. (6) and (7), we see that $P_S > P_B$ requires that

$$\rho_S\kappa_S^2I_1(r_T/\kappa_S) > \rho_S\kappa_B^2I_2(r_T/\kappa_B, H/\kappa_B) \Leftrightarrow \frac{\kappa_S^2}{\kappa_B^2} > \frac{I_2(r_T/\kappa_B, H/\kappa_B)}{I_1(r_T/\kappa_S)}. \quad (10)$$

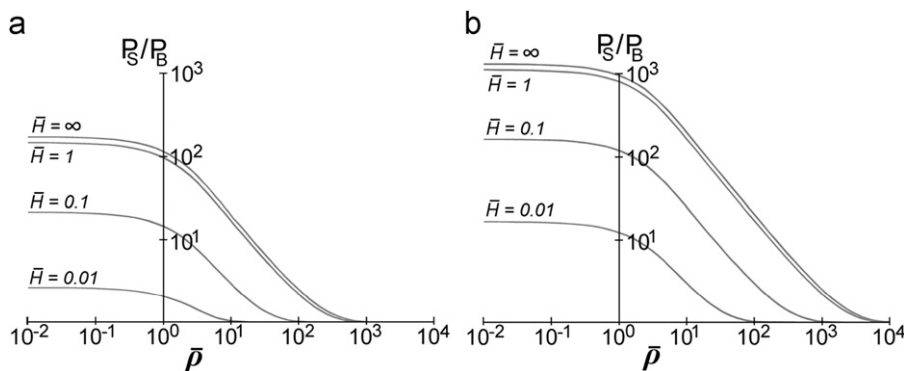


Fig. 3. The dependence of the ratio of surface and bulk encounter probabilities, P_S/P_B , on the nondimensional target density, $\bar{\rho}$, for relative target size (a) $r = 10^{-3}$ and (b) $r = 10^{-4}$, and various relative water depths \bar{H} . Here $r = r_T/\kappa$, $\bar{H} = H/\kappa$ and $\bar{\rho} = \kappa^2\rho_S$, where r_T, H, ρ_S are the target size, water depth and target density, and $\kappa = \sqrt{D/\lambda}$ is the gamete range, where λ is the loss rate and D is the gamete diffusivity. The ratio P_S/P_B approaches 1 for high target density $\bar{\rho}$, but the typical density at which this happens increases with the water depth \bar{H} . For small target density, the ratio P_S/P_B is independent of the density.

We now nondimensionalize as in the previous case, setting $r = r_T/\kappa_S$, $\bar{H} = H/\kappa_S$ and $\mu = \kappa_S/\kappa_B$. Thus μ is the ratio of the gamete ranges on the surface and in the bulk, and hence indicates how favourable the conditions are for random walk encounters on the surface relative to the bulk. As we might expect the conditions to be more favourable in the bulk due to lower predation, one might expect $\kappa_B > \kappa_S$, so $\mu = \kappa_S/\kappa_B < 1$. The criterion (10) then transforms to

$$P_S > P_B \Leftrightarrow I_1(r)\mu^2 > I_2(\mu r, \mu\bar{H}) \quad (11)$$

with $I_1(r) = 2\pi/K_0(r) \int_r^\infty xK_0(x) dx$ and $I_2(r, s) = 2\pi/A(r, s) \int_r^\infty xA(x, s) dx$.

The curves of $P_S = P_B$ are shown graphically in Fig. 4 for three typical values of r and a range of μ and \bar{H} . We observe that for smaller relative target size r the surface search becomes more advantageous. For small values of \bar{H} , the critical value of μ , for which $P_S = P_B$, is close to 1, whereas for large \bar{H} the critical value of μ converges to a constant that decreases linearly with r .

3.3. Anisotropic diffusion

So far, we have compared the cases of search in the fluid bulk and on the surface. However, in many cases the particles are not strictly constrained to the surface but rather to a region just beneath it. This is the case, for example, for light-sensitive motile gametes or for buoyant particles in turbulent waters. Since we have shown that $P_B \approx P_S$ when $H \rightarrow r_T$, if the depth of this region is

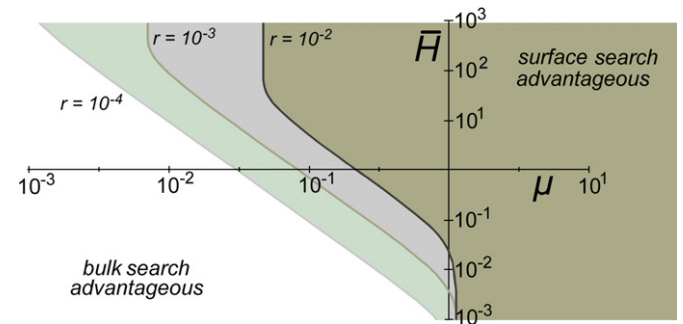


Fig. 4. Log-log graph of the critical relative water depth $\bar{H} = H/\kappa_S$ at which surface and bulk searches are equally advantageous ($P_S = P_B$) as a function of $\mu = \sqrt{(\lambda_B/\lambda_S)(D_S/D_B)}$, for different values of $r = r_T/\kappa_S$. Here, H is the water depth, r_T the target size and $\kappa_S = \sqrt{D_S/\lambda_S}$, with λ_S, λ_B and D_S, D_B being the loss rates and diffusivities on the surface and in the bulk, respectively. Only when loss rates are greatly enhanced at the surface (small μ), and for shallow domains (small \bar{H}), is bulk search advantageous.

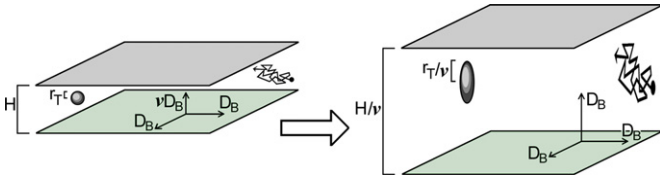


Fig. 5. Rescaling vertical distances by ν , the relative magnitude of vertical and horizontal diffusivities, allows our model to capture the influence of anisotropic diffusion.

comparable to the target size, or if the depth of this region is much smaller than the total water depth, we can treat this case just like the surface search. When the depth H_2 of the region in which the gametes move cannot be considered much smaller than the total depth H , we have to compare $P_B(\rho_S, H, r_T, \kappa_B)$ and $P_B(\rho_S, H_2, r_T, \kappa_B)$. We expect the same qualitative features to apply here as in the previous cases, though we expect the magnitude of the differences between the two scenarios (near-surface and fluid bulk) to be smaller.

So far, we have assumed that the diffusion of the particles happens isotropically. However, this is not always the case. For example, turbulent mixing near the surface is typically anisotropic, with different magnitudes in the horizontal and vertical directions. Typically, convective currents in the bulk enhance the vertical component of turbulent mixing, while the presence of a free surface decreases it. Similarly, we expect phototactic gametes to move preferentially in the horizontal plane rather than the vertical once they reach the surface. Such anisotropy affects our treatment of the 3D search, both for the whole fluid bulk and for the near-surface region. Let us suppose then, that instead of isotropic diffusion with diffusivity D_B , we have anisotropic diffusion with horizontal and vertical diffusivities D_H and D_V , respectively. If we write $D_V = \nu D_H$, then we can convert this case to one almost identical to the one already studied just by rescaling all the vertical dimensions by ν (see Fig. 5). The reason why we do not get exactly the familiar scenario is that now the target is an ellipsoid with vertical semi-axis of length r_T/ν instead of a sphere. We would like to replace it with a sphere of radius r_T^* which is equally likely to be encountered. A reasonable approximation for small r_T is a sphere of roughly the same surface area. Approximating the surface of the ellipsoid to be $4\pi r_T^2/\nu$ yields $r_T^* = r_T/\sqrt{\nu}$. Therefore with anisotropic diffusion, we should evaluate $P_B(\rho_S, H/\nu, r_T/\sqrt{\nu}, \kappa_B)$ instead of $P_B(\rho_S, H, r_T, \kappa_B)$. It is apparent that when $\nu < 1$, this should increase P_B since the particles then move less in the vertical direction and thus the random walk is closer to planar.

4. Discussion

We proceed by applying our results to three specific biological systems. Relevant parameters for each system are listed in Table 2. First, for a typical coral we assume the gamete diffusion to be mainly due to the fluid motion. Both the surface turbulence and currents near the bottom have typical speed $U = 0.1$ m/s and scale $L = 0.1$ m, giving a diffusivity $D \approx 10^{-2}$ m²/s. As the gametes survive for many hours after release, the loss rate $\lambda < 10^{-4}$ s⁻¹. We here consider the worst case scenario $\lambda = 10^{-4}$ s⁻¹. Referring to Table 2 and Fig. 6, we see that bulk search would be advantageous only for $\mu < 0.03$, which corresponds to the loss rate being 1000 times larger on the surface than in the bulk. Hence, we expect the surface search to be advantageous for all realistic values of loss rates and diffusivities, an inference consistent with the fact that many coral species do employ the water surface for their reproduction (Oliver and Babcock, 1992). We discuss below

Table 2

Values of relevant parameters for three types of water-dwelling organisms. The critical value of μ , the relative hostility of the surface environment required to cancel the advantage gained by surfacing, is found to be high for corals and the marine algae *M. angicava*, and low for the annelid worm *P. californica*. As expected, organisms living in conditions where μ is high (e.g. *M. angicava* and a large number of coral species) tend to employ the water surface for reproduction, while those with low μ employ the water bulk (e.g. *P. californica*).

	Typical coral	<i>M. angicava</i>	<i>P. californica</i>
Depth [m]	10	0.4	0.25
Target size r_T [mm]	1	0.01	5
Diffusivity D [m ² s ⁻¹]	10^{-2}	2×10^{-8}	10^{-5}
Loss rate λ [s ⁻¹]	10^{-4}	2×10^{-4}	10^{-4}
Gamete range κ_S [m]	10	0.01	0.5
Rel. target size r	10^{-4}	10^{-3}	10^{-2}
Rel. depth \bar{H}	1	40	0.5
Crit. value of μ	0.03	0.02	0.3

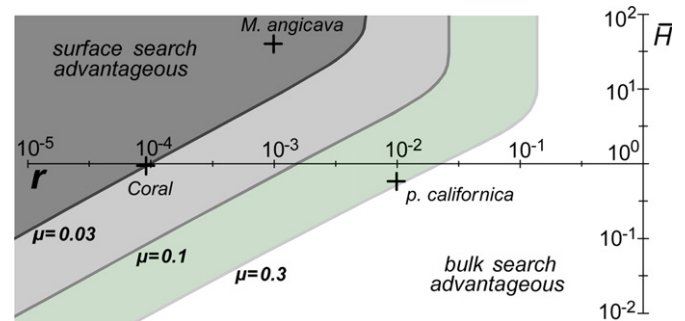


Fig. 6. Log-log plot of the critical value of relative water depth $\bar{H} = H/\kappa_S$, at which surface and bulk searches are equally advantageous ($P_S = P_B$), as a function of relative target size $r = r_T/\kappa_S$, for different values of $\mu = \sqrt{(\lambda_B/\lambda_S)(D_S/D_B)}$. Here, H is the water depth, r_T the target size and $\kappa_S = \sqrt{D_S/\lambda_S}$ the range, with λ_S , λ_B and D_S , D_B being the loss rates and diffusivities on the surface and in the bulk, respectively. Three example organisms are shown in the graph. For fixed r and \bar{H} , one can read off the maximum value of μ for which the advantage of surface search is outweighed by surface environment hostility. Surface search is more efficient for corals and *M. angicava* when $\mu > 0.03$, and for *P. californica* when $\mu > 0.3$.

why some species do not use this strategy despite the robust advantage predicted by our model.

Second, marine green alga *Monostroma angicava* has phototactic gametes that concentrate near the water surface. Their typical gamete speed is 2×10^{-4} m/s and tumbling timescale 5×10^{-1} s, giving a diffusivity $D = 2 \times 10^{-8}$ m²/s. We estimate the dimensional loss rate to be on the order of 2×10^{-4} s⁻¹ (i.e. more than half of the gametes will be dead after 2 h, see Grave and Oliphant, 1930). From Table 2 and Fig. 6, we infer that a surface to bulk loss rate ratio of at least 5000 is required to favour the bulk search. Hence, surface search is again favourable.

Third, we consider the case of a polychaete annelid worm *Phragmatopoma californica*, which does not employ surface search. We obtain a critical value of $\mu \approx 0.3$, so indeed, in this scenario the advantage of surfacing can be easily outweighed by relatively hostile surface conditions. The main difference between this and the previous two examples is the large size of the annelid gametes relative to their range, which accounts for their use of the bulk search.

The results of our analysis suggest that surface search is advantageous in a variety of situations spanning a broad range of scales. However, we have thus far tacitly assumed that organisms release their gametes onto the same surface on which they themselves live. Many bottom-dwelling organisms nevertheless release positively buoyant gametes, which float to the

water surface. Getting to the surface might be a long and dangerous process, especially in deep water. If the male gametes have any means of detecting the location of female gamete (e.g. chemotaxis), this may also negate the disadvantage of the 3D random walk. There are many other ways in which organisms can tweak the encounter probability in the right direction; however, as this can be typically be done both on the surface and in the bulk, this introduces complications beyond the scope of our model. For example, deep dwelling organisms release their gametes with significant initial velocity, which hastens their spread. Flowers on the water surface use surface tension to distort the neighbouring free surface and thus increase their effective target size. The maximum increase in the target radius attainable by this method is twice the capillary length $l_c = \sqrt{\sigma/\rho g} \approx 2$ mm, which can increase the surface encounter probability substantially for small gametes.

Under most conditions, the encounter rates between passive particles are higher on or near the surface than within the bulk. This geometric consequence may have some bearing on models of the creation of early terrestrial life. According to most current theories, the simple organic molecules created by natural processes in the atmosphere and oceans (Miller, 1953) accumulated on the water surface, and were possibly further concentrated near the shores by wind (Panno, 2004), there combining to form macromolecules capable of replication and metabolism. Although the mechanism responsible remains a point of contention, it is clear that constraining the basic molecules to lie on a surface would significantly increase the encounter rate, thus accelerating the process. We note that other factors might have further concentrated these molecules, for example containment within bubbles or drops created by breaking waves or hydrothermal vents. In any case, our study suggests that the evolution of early life would have been accelerated had it arisen on the water surface.

Increased encounter rates near surfaces can also affect how we interpret reproduction in liverworts and hornworts, “lower” plants thought to be similar to those that first invaded the terrestrial environment. Because liverworts and hornworts require a film of liquid water as a pathway by which antherozoids are delivered to eggs, reproduction in the terrestrial environment is considered to be at a disadvantage relative to that in water. However, confinement to a thin film of water might actually increase the probability of antherozoid–egg encounter relative to that operating when antherozoids are dispersed into a lake or stream.

Finally, our model points in the direction of novel models of predator–prey dynamics. Predatory habits will generally depend on the type of region to which movement is confined. Presumably different strategies will be required for catchment of prey moving on a surface than in the bulk. While predators and prey are often confined to the same fluid domain, such is not always the case; for example, some birds prey on fish only at or near the water surface. The role of geometry on predator–prey dynamics is left as a subject for future research.

Appendix A. Exact solutions for \bar{P}_d in infinite geometries

Consider two motile gametes (point particles) performing random walks in d -dimensional space. Let the lengthscales of the random walk steps be δ_1 and δ_2 for the first and second gamete, respectively, and the timescale of the step be τ , common for both. Also let the loss rates for each gamete be λ_1 , λ_2 , respectively. Now let \bar{P}_d be the probability that the gametes will ever encounter each other, that is, that they will get within a distance r_T of each other before expiring. Only the distance

between the gametes and the loss rates λ_1 , λ_2 play a role in this probability, so $\bar{P}_d = \bar{P}_d(R, \lambda_1, \lambda_2)$ where $R = |\mathbf{x}_1 - \mathbf{x}_2|$. We can choose the coordinates so that at time $t=0$ one gamete is at the origin and the other one is at $R\hat{\mathbf{e}}_x$. Considering the encounter probability at time $t = \tau$, we arrive at

$$\bar{P}_d(R) = (1 - \lambda_1\tau)(1 - \lambda_2\tau) \frac{1}{(S_d)^2} \int_{S_d} d\mathbf{m} \int_{S_d} d\mathbf{n} \bar{P}_d(|R\hat{\mathbf{e}}_x + \delta_1\mathbf{m} - \delta_2\mathbf{n}|), \quad (\text{A.1})$$

where S_d is the surface of a d -dimensional sphere and \mathbf{m} , \mathbf{n} are unit vectors. Writing $\mathbf{r} = \delta_1\mathbf{m} - \delta_2\mathbf{n}$ and assuming $r \ll R$ (i.e. $\delta_1 \ll R$ and $\delta_2 \ll R$), Taylor series expansion yields

$$\bar{P}_d(R) = (1 - \lambda_1\tau)(1 - \lambda_2\tau) \left[\bar{P}_d(R) + \left(\frac{\delta_1^2 + \delta_2^2}{2R} - \frac{\delta_1^2 + \delta_2^2}{2Rd} \right) \bar{P}'_d(R) + \frac{\delta_1^2 + \delta_2^2}{2d} \bar{P}''_d(R) + O\left(\frac{r^2}{R^2}\right) \right]. \quad (\text{A.2})$$

Writing $D = (\delta_1^2 + \delta_2^2)/2d\tau$, $\lambda = \lambda_1 + \lambda_2$, and letting $\delta_1 \rightarrow 0$, $\delta_2 \rightarrow 0$ and $\tau \rightarrow 0$ while keeping D and λ constant simplifies Eq. (A.2) to

$$\bar{P}_d(R) = \kappa^2 \left[\frac{d-1}{R} \bar{P}'_d(R) + \bar{P}''_d(R) \right], \quad (\text{A.3})$$

where $\kappa^2 = D/\lambda$. The boundary conditions are

$$\bar{P}_d(r_T) = 1 \quad \text{and} \quad \lim_{R \rightarrow \infty} \bar{P}_d(R) = 0. \quad (\text{A.4})$$

ODE (A.3) can be easily solved for both $d=2$ and $d=3$; applying the boundary conditions (A.4) we get

$$\begin{aligned} \bar{P}_2(R) &= \frac{K_0(R/\kappa)}{K_0(r_T/\kappa)} = \frac{K_0(\sqrt{\lambda R^2/D})}{K_0(\sqrt{\lambda r_T^2/D})}, \\ \bar{P}_3(R) &= \frac{r_T}{R} e^{-(R-r_T)/\kappa} = \frac{r_T \exp\{\sqrt{\lambda r_T^2/D}\}}{\text{Rexp}\{\sqrt{\lambda R^2/D}\}}, \end{aligned} \quad (\text{A.5})$$

where $K_0(s)$ is the modified Bessel functions of the second kind of order zero.

Appendix B. Encounter probability in finite-depth 3D scenario

When the body of water has a finite depth H , we cannot use the spherical symmetry which allowed us to treat the encounter probability as a function of the initial gamete distance only. We will use a less direct method based on manipulations of the probability density function $f(\mathbf{x}, t)$ describing the location of a gamete. For simplicity, we will assume one gamete (the target) to be non-motile and place it at the origin of our coordinate system. The integral of $f(\mathbf{x}, t)$ over the whole space gives us the probability that the motile gamete is still alive at time t . Introduction of an absorbing boundary condition at the encounter distance from the target (i.e. distance r_T from the origin) further reduces the total integral of $f(\mathbf{x}, t)$, by an amount which must be equal to the encounter probability between the two gametes.

We proceed by deriving the evolution equation for $f(\mathbf{x}, t)$ and then solving it under the initial and boundary conditions of the two- and three-dimensional scenarios.

B.1. Evolution of $f(\mathbf{x}, t)$

Consider the evolution of the PDF $f(\mathbf{x}, t)$ for a particle performing a random walk in d -dimensional space. We assume that the particle moves in discrete steps of length δ , each step takes time τ and the loss rate is λ , i.e. over a timestep τ , f is reduced by an amount $\lambda\tau f$. The direction of each step is random and every direction is equally

likely. If the particle is at \mathbf{x} at time t , at time $t-\tau$ it must have been at a point $\hat{\mathbf{x}}$ with $|\mathbf{x}-\hat{\mathbf{x}}| = \delta$. Hence if we average the PDF at all such points, we will get the PDF at \mathbf{x} and t . In d dimensions (S_d is the surface of the d -dimensional unit sphere)

$$f(\mathbf{x}, t) = \frac{1-\lambda\tau}{S_d} \int_{S_d} f(\mathbf{x} + \delta\mathbf{n}, t-\tau) dS_d. \quad (\text{B.1})$$

Assuming δ small and using the symmetry of S_d , Taylor expansion of the right-hand side of (B.1) yields

$$f(\mathbf{x}, t) = (1-\lambda\tau) \left[f(\mathbf{x}, t-\tau) + \frac{\delta^2}{2d} \nabla^2 f(\mathbf{x}, t-\tau) + O(\delta^3) \right]. \quad (\text{B.2})$$

Writing $D = \delta^2/2\tau d$ and letting $\tau \rightarrow 0$ and $\delta \rightarrow 0$ while keeping D fixed yields

$$\frac{\partial f}{\partial t} = D \nabla^2 f - \lambda f. \quad (\text{B.3})$$

B.2. 2D absorption

We want to solve the evolution Eq. (B.3) subject to the initial condition $f(\mathbf{x}, 0) = \delta(\mathbf{x}-\mathbf{x}_0)$ and the absorbing boundary condition $f(\mathbf{x}, t) = 0$ on $|\mathbf{x}| = r_T$. Letting $R = |\mathbf{x}_0|$ and nondimensionalizing using

$$\mathbf{x} = R\hat{\mathbf{x}}, \quad t = \frac{R^2}{D}\hat{t}, \quad r_T = R\epsilon, \quad \lambda = \frac{\lambda D}{R^2}, \quad (\text{B.4})$$

we transform the system into

$$\frac{\partial f}{\partial \hat{t}} = \hat{\nabla}^2 f - \hat{\lambda} f \quad \text{for } \hat{t} \geq 0,$$

$$f(\hat{\mathbf{x}}, 0) = \delta(\hat{\mathbf{x}} - \hat{\mathbf{x}}_0),$$

$$f(\hat{\mathbf{x}}, \hat{t}) = 0 \quad \text{for } |\hat{\mathbf{x}}| = \epsilon. \quad (\text{B.5})$$

Without the absorbing boundary condition and with $\hat{\lambda} = 0$, f would be given simply by

$$f(\hat{\mathbf{x}}, \hat{t}) = \frac{1}{4\pi\hat{t}} e^{-|\hat{\mathbf{x}}-\hat{\mathbf{x}}_0|^2/4\hat{t}}. \quad (\text{B.6})$$

Now since the governing equation in (B.5) is linear, the solution to the full system will be given by the sum of (B.6) and a corrector function $f_c(\hat{\mathbf{x}}, \hat{t})$, whose value at $|\hat{\mathbf{x}}| = \epsilon$ will be exactly the opposite of the value of (B.6) there, so together they satisfy the boundary condition. Assuming $\epsilon \ll 1$, the variation of Eq. (B.6) over the circle $|\hat{\mathbf{x}}| = \epsilon$ will be always small relative to its value, so we can approximate it by its value at the origin. This means that our approximation to f_c (call it \tilde{f}_c) has to satisfy radially symmetric boundary condition $\tilde{f}_c(\hat{\mathbf{x}}, \hat{t}) = -f(0, \hat{t})$ at $|\hat{\mathbf{x}}| = \epsilon$. Therefore \tilde{f}_c will be radially symmetric: $\tilde{f}_c(\hat{\mathbf{x}}, \hat{t}) = \tilde{f}_c(r, \hat{t})$. We can thus write the general form of $\tilde{f}_c(r, \hat{t})$ satisfying I.C. $\tilde{f}_c(r, 0) = 0$

$$\tilde{f}_c(r, \hat{t}) = - \int_0^{\hat{t}} A_2(u) \frac{e^{-r^2/4(\hat{t}-u)}}{4\pi(\hat{t}-u)} du \quad (\text{B.7})$$

and it must satisfy the boundary condition at $|\hat{\mathbf{x}}| = \epsilon$

$$-\tilde{f}_c(\epsilon, \hat{t}) = f(0, \hat{t}) = \frac{e^{-|\hat{\mathbf{x}}_0|^2/4\hat{t}}}{4\pi\hat{t}} = \frac{e^{-1/4\hat{t}}}{4\pi\hat{t}}. \quad (\text{B.8})$$

We can visualize \tilde{f}_c as continually releasing “particles” at the origin. From now on we will drop the hats on the nondimensionalized time.

Hence our approximate solution to (B.5) is

$$f(\mathbf{x}, t) = \frac{e^{-|\mathbf{x}-\mathbf{x}_0|^2/4t}}{4\pi t} - \int_0^t A_2(u) \frac{e^{-\mathbf{x}^2/4(t-u)}}{4\pi(t-u)} du. \quad (\text{B.9})$$

In order for Eq. (B.9) to satisfy Eq. (B.8), we must have

$$\int_0^t A_2(u) \frac{e^{-\mathbf{x}^2/4(t-u)}}{4\pi(t-u)} du = \frac{e^{-1/4t}}{4\pi t}, \quad \forall t \geq 0. \quad (\text{B.10})$$

The total encounter (absorption) probability is given by

$$\bar{P}_2 = \int_0^\infty A_2(u) du, \quad (\text{B.11})$$

where $A_2(x)$ is determined for all $x \geq 0$ by the relation (B.10). If we now have non-zero $\hat{\lambda}$ in Eq. (B.5), we can proceed in a similar manner as above, inserting factors of $e^{-\hat{\lambda}t}$ where necessary to finally arrive at Eq. (B.11) again, but this time with $A_2(x)$ determined by

$$\int_0^t A_2(u) K_2(t-u, \hat{\lambda}, \epsilon) du = K_2(t, \hat{\lambda}, 1) \quad \text{for } \forall t \geq 0, \quad (\text{B.12})$$

where $K_2(x, \hat{\lambda}, \epsilon) = 1/x e^{-\hat{\lambda}x - \epsilon^2/4x}$.

We can compute $\bar{P}_2(\hat{\lambda}, \epsilon)$ by integrating Eq. (B.12) from 0 to ∞ with respect to t and using Eq. (B.11) to obtain

$$\bar{P}_2(\hat{\lambda}, \epsilon) = \frac{\int_0^\infty K_2(u, \hat{\lambda}, 1) du}{\int_0^\infty K_2(u, \hat{\lambda}, \epsilon) du} = \frac{\int_0^\infty \frac{1}{u} e^{-\hat{\lambda}u - 1/4u} du}{\int_0^\infty \frac{1}{u} e^{-\hat{\lambda}u - \epsilon^2/4u} du}. \quad (\text{B.13})$$

B.3. 3D absorption

We proceed just as in the 2D case, starting from the system (dropping the hats and writing $\alpha = H/R$)

$$\frac{\partial f}{\partial t} = \nabla^2 f - \lambda f \quad \text{for } t \geq 0, \quad f(\mathbf{x}, 0) = \delta(\mathbf{x}-\mathbf{x}_0), \quad f(\mathbf{x}, t) = 0 \quad \text{for } |\mathbf{x}| = \epsilon, \quad (\text{B.14})$$

$$\frac{\partial f}{\partial z} = 0 \quad \text{at } z = 0 \quad \text{and } z = \alpha, \quad (\text{B.15})$$

only this time, the solution with $\hat{\lambda} = 0$, without absorbing boundary condition and without the reflecting surfaces at $z=0$ and $z=\alpha$ would be given by

$$f(\mathbf{x}, t) = \frac{e^{-|\mathbf{x}-\mathbf{x}_0|^2/4t}}{(4\pi t)^{3/2} t^{3/2}}, \quad (\text{B.16})$$

where $\mathbf{x}_0 = (1, 0, 0)$.

In order to get rid of the boundary conditions at $z=0$ and $z=\alpha$, we reflect the point \mathbf{x}_0 and the absorbing surface in both planes infinitely many times (see Fig. 7), so that they are satisfied

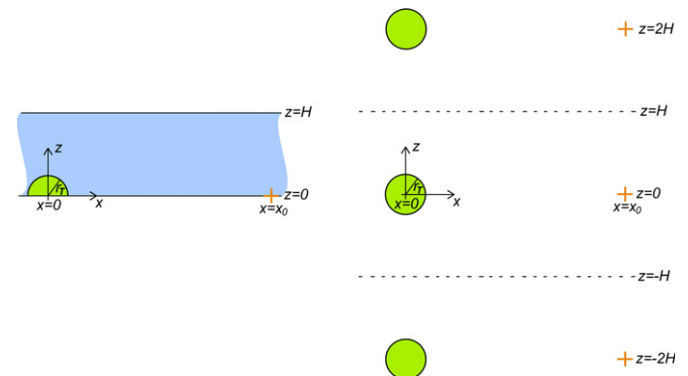


Fig. 7. Left: original setup in the finite 3D scenario. Right: after performing reflections in both planes.

automatically by symmetry

$$f(\mathbf{x}, t) = \frac{1}{(4\pi)^{3/2} t^{3/2}} \left[\sum_{n=-\infty}^{\infty} e^{-|\mathbf{x}-\mathbf{x}_n|^2/4t} \right], \quad (B.17)$$

where $\mathbf{x}_n = (1, 0, z_n)$ with $z_n = 2n\alpha$. Again the situation is symmetrical about both $z=0$ and $z=\alpha$ so the reflecting boundary conditions are met. Now we have to consider the absorbing boundary at the origin and all its reflections (centered at $(0, 0, z_n)$). Since $\epsilon \ll 1$, just as previously we can introduce a corrector function f_c , which is now a superposition of a spherically symmetric function about the origin and all its reflections in the planes. Due to the symmetry of the situation, if we satisfy the boundary condition on one of the absorbing surfaces (say the one around the origin) then we will automatically satisfy the boundary condition on all of its reflections too. Hence our approximate solution to the whole system (B.14) and (B.15) is given by

$$f(\mathbf{x}, t) = \frac{1}{(4\pi)^{3/2}} \left[\frac{1}{t^{3/2}} \sum_{n=-\infty}^{\infty} e^{-|\mathbf{x}-\mathbf{x}_n|^2/4t} - \sum_{n=-\infty}^{\infty} \int_0^t A_3(u) \frac{e^{-|\mathbf{x}-\mathbf{x}_n|^2/4(t-u)}}{(t-u)^{3/2}} du \right], \quad (B.18)$$

where $\mathbf{x}'_n = (0, 0, z_n)$, subject to $f(\epsilon \mathbf{n}, t) = 0$, i.e.

$$\sum_{n=-\infty}^{\infty} \int_0^t A_3(u) \frac{e^{-(\epsilon^2 + z_n^2)/4(t-u)}}{(t-u)^{3/2}} du = \frac{1}{t^{3/2}} \sum_{n=-\infty}^{\infty} e^{-(1+z_n^2)/4t}. \quad (B.19)$$

Then our encounter (absorption) probability function is $\bar{P}_{3F} = \int_0^\infty A_3(u) du$. If we denote $S(x) = \sum_{n=-\infty}^{\infty} e^{-x n^2}$, then $\sum_{n=-\infty}^{\infty} e^{-z_n^2/4t} = \sum_{n=-\infty}^{\infty} e^{-2n\alpha^2/4t} = S(\alpha^2/t)$. Now going back to non-zero $\hat{\lambda}$, we can go through the same steps as above, inserting factors of $e^{-\hat{\lambda}t}$ where appropriate to arrive at a modified version of Eq. (B.19)

$$\int_0^t A_3(u) K_3(t-u, \hat{\lambda}, \epsilon) du = K_3(t, \hat{\lambda}, 1), \quad \forall t \geq 0,$$

where

$$K_3(x, \hat{\lambda}, \epsilon) = \frac{e^{-\hat{\lambda}x - \epsilon^2/4x}}{x^{3/2}} S\left(\frac{\alpha^2}{x}\right) \quad \text{for } x \geq 0. \quad (B.20)$$

Integrating Eq. (B.20) from 0 to ∞ , and employing the same method as in the 2D case, we eventually arrive at

$$\bar{P}_{3F}(\hat{\lambda}, \epsilon, \alpha) = \frac{\int_0^\infty K_3(u, \hat{\lambda}, 1) du}{\int_0^\infty K_3(u, \hat{\lambda}, \epsilon) du} = \frac{\int_0^\infty u^{-3/2} e^{-\hat{\lambda}u - 1/4u} S\left(\frac{\alpha^2}{u}\right) du}{\int_0^\infty u^{-3/2} e^{-\hat{\lambda}u - \epsilon^2/4u} S\left(\frac{\alpha^2}{u}\right) du} \quad (B.21)$$

It can be shown that the formulae (B.13) and (B.21) are actually exactly equal to the exact expressions (A.5) for infinite geometries (i.e. when $\alpha = \infty$ in 3D scenario), by showing that they satisfy the same ODE with the same boundary conditions. Using Eq. (A.5) in Eq. (B.21) allows us to simplify (B.21) to

$$\bar{P}_3(\hat{\lambda}, \epsilon, \alpha) = \frac{\sum_{n \in Z} \frac{e^{-\sqrt{(1+4n^2\alpha^2)\hat{\lambda}}}}{\sqrt{1+4n^2\alpha^2}}}{\sum_{n \in Z} \frac{e^{-\sqrt{(\epsilon^2+4n^2\alpha^2)\hat{\lambda}}}}{\sqrt{\epsilon^2+4n^2\alpha^2}}}. \quad (B.22)$$

Appendix C. Continuum of gametes

Consider the case of infinite 2- or 3-dimensional space filled uniformly with targets (female gametes). Let the target density,

i.e. the probability of finding a target within a small region divided by the region volume, be ρ_2 in 2D scenario and ρ_3 in 3D scenario. We can then place a particle (a male gamete) in this continuum of targets and ask what is the probability P_S, P_B , that it will encounter a female gamete before it dies, in 2D and 3D, respectively. We can obtain P_S and P_B using the known encounter probabilities $\bar{P}_2(R), \bar{P}_3(R)$ for a pair of gametes a distance R apart, in 2D and 3D, respectively (see Appendix A).

In 2D, divide the plane into concentric rings of thickness δr around the male gamete. The probability of finding a female gamete in a ring with radius r is $(2\pi r \delta r) \rho_2$ and the probability that the male gamete will not encounter a female gamete originating from this ring is then $1 - (2\pi r \delta r) \rho_2 \bar{P}_2(r)$. Hence the total probability of the male gamete not encountering any female gamete is then $1 - P_S = \prod_{n=0}^{\infty} [1 - (2\pi(n\delta r) \delta r) \rho_2 \bar{P}_2(n\delta r)]$. Taking the logarithm of both sides yields $\ln(1 - P_S) = \sum_{n=0}^{\infty} \ln[1 - (2\pi(n\delta r) \delta r) \rho_2 \bar{P}_2(n\delta r)]$ and taking the limit $\delta r \rightarrow 0$ gives $\ln(1 - P_S) = \int_0^\infty \ln[1 - 2\pi r \delta r \rho_2 \bar{P}_2(r)] = \int_0^\infty -2\pi r \delta r \rho_2 \bar{P}_2(r) = -\rho_2 \int_0^\infty 2\pi r \bar{P}_2(r) dr$. Since the gametes must be at least a distance r_T apart originally (the sum of their radii), we can integrate from r_T instead of 0. Thus we obtain

$$P_S = 1 - \exp\left\{-\rho_2 \int_{r_T}^{\infty} 2\pi r \bar{P}_2(r) dr\right\}. \quad (C.1)$$

Similarly, in 3D we find

$$P_B = 1 - \exp\left\{-\rho_3 \int_{r_T}^{\infty} 2\pi r \bar{P}_{3F}(r) dr\right\}. \quad (C.2)$$

References

Adam, G., Delbrück, M., 1968. Reduction of dimensionality in biological diffusion processes. In: Structural Chemistry and Molecular Biology, W.H. Freeman and Company, San Francisco/London, pp. 198–215.

Berg, H.C., 1993. In: Random Walks in Biology, Princeton University Press, pp. 6–12.

Cox, P.A., Knox, R.B., 1988. Pollination postulates and two-dimensional pollination in hydrophilous monocotyledons. Ann. MO Bot. Gard. 75, 811–818.

Cox, P.A., 1983. Search theory, random motion, and the convergent evolution of pollen and spore morphology in aquatic plants. Am. Nat. 121, 9–31.

Crimaldi, J.P., Browning, H.S., 2004. A proposed mechanism for turbulent enhancement of broadcast spawning efficiency. J. Mar. Syst. 49, 3–8.

Denny, M.W., 1988. Biology and the Mechanics of the Wave-Swept Environment. Princeton University Press.

Denny, M.W., 1994. Air and Water Princeton University Press.

Denny, M.W., Shibata, M.F., 1989. Consequences of surf-zone turbulence for settlement and external fertilization. Am. Nat. 134, 859–889.

Grave, B.H., Oliphant, J.F., 1930. The longevity of unfertilized gametes. Biol. Bull. 59, 233–239.

Harrison, P.L., Babcock, R.C., Bull, G.D., Oliver, J.K., Wallace, C.C., Wallis, B.L., 1984. Mass spawning in tropical reef corals. Science 223, 1186–1189.

Levitan, D.R., Petersen, C., 1995. Sperm limitation in the sea. Trends Ecol. Evol. 10, 228–231.

Miller, S.L., 1953. Production of amino acids under possible primitive earth conditions. Science 117, 528.

Oliver, J., Babcock, R., 1992. Aspects of the fertilization ecology of broadcast spawning corals: sperm dilution effects and in situ measurements of fertilization. Biol. Bull. 183, 409–417.

Panno, J., 2004. The Cell: Evolution of the First Organism (New Biology). Facts on File (pp. 11–15).

Pearse, J.S., McClary, D.J., Sewell, M.A., Austin, W.C., Perez-Ruzafa, A., Byrne, M., 1988. Simultaneous spawning of six species of echinoderms in Barkely Sound, British Columbia. Invertebr. Reprod. Dev. 14, 279–288.

Pearson, G.A., Brawley, S.H., 1996. Reproductive ecology of *Fucus distichus* (L.): an intertidal alga with external fertilization. Mar. Ecol. Prog. Ser. 143, 211–223.

Santelices, B., 2002. Recent advances in fertilization ecology of macroalgae. J. Phycol. 38, 4–10.

Togashi, T., Cox, P.A., 2001. Tidal-linked synchrony of gamete release in the marine green alga, *Monostroma angicava* Kjellman. J. Exp. Mar. Biol. Ecol. 264, 117–131.